J Neuropathol Exp Neurol
Vol. 76, No. 8, August 2017, pp. 665–675
doi: 10.1093/jnen/nlx047

ORIGINAL ARTICLE

Heart and Nervous System Pathology in Compound Heterozygous Friedreich Ataxia

Alyssa B. Becker, BA, Jiang Qian, MD, PhD, Benjamin B. Gelman, MD, PhD, Michele Yang, MD, Peter Bauer, MD, and Arnulf H. Koeppen, MD

Abstract

In a small percentage of patients with Friedreich ataxia (FA), the pathogenic mutation is compound heterozygous, consisting of a guanine–adenine–adenine (GAA) trinucleotide repeat expansion in one allele, and a deletion, point mutation, or insertion in the other. In 2 cases of compound heterozygous FA, the GAA expansion was inherited from the mother, and deletions from the father. Compound heterozygous FA patient 1, an 11-year-old boy (GAA, 896/c.11_12TCdel), had ataxia, chorea, cardiomyopathy, and diabetes mellitus. Compound heterozygous FA patient 2, a 28-year-old man (GAA, 744/exon 5 del), had ataxia, cardiomyopathy, and diabetes mellitus. Microscopy showed cardiomyocyte hypertrophy, iron-positive inclusions, and disrupted intercalated discs. The cardiac lesions were similar to those in age-matched homozygous FA patients with cardiomyopathy and diabetes mellitus (boy, 10, GAA 1016/1016; woman, 25, GAA 800/1100). The neuropathology was also similar and included hypoplasia of spinal cord and dorsal root ganglia, loss of large axons in dorsal roots, and atrophy of the dentate nucleus (DN). Frataxin levels in heart and DN of all 4 FA cases were at or below the detection limits of the enzyme-linked immunosorbent assay ($\leq$10 ng/g wet weight) (normal DN: 126 $\pm$ 43 ng/g; normal heart: 266 $\pm$ 92 ng/g). The pathologic phenotype in homozygous and compound heterozygous FA is determined by residual frataxin levels rather than unique mutations.

Key Words: Cardiomyopathy, Compound heterozygosity, Dentate nucleus, Dorsal root ganglion, Frataxin, Friedreich ataxia.

INTRODUCTION

In the vast majority of patients with Friedreich ataxia (FA), the pathogenic mutation is a guanine–adenine–adenine (GAA) trinucleotide repeat expansion in intron 1 of the frataxin gene (*FXN*) (1). In a small percentage of patients, however, FA is caused by a GAA expansion in one allele and a point mutation, deletion, or insertion in the other (2). The clinical phenotype of compound heterozygotes, including age of onset, cardiomyopathy, or diabetes mellitus appears to depend on the predicted residual level of frataxin (2). This report presents the neural and cardiac pathology in 2 compound heterozygous FA patients and 2 homozygous FA patients, and compares the findings with age-matched normal controls. Both heterozygous FA patients had inherited a GAA trinucleotide repeat expansion from their mothers and a deletion from their fathers. The observations confirmed the conclusion that impaired *FXN* transcription, or biosynthesis of an unstable or truncated protein from the modified alleles, determines the pathologic phenotype of FA (2–4).

Case Reports

Compound Heterozygous FA Case 1, Boy, 11. The patient was born at 35 weeks gestation. He weighed 2466 g at birth and was 46 cm long. His mother noticed that his motor and language skills in early childhood did not develop at the same pace as in his 3 brothers. At the age of 5 years, an occupational therapist also observed an unusual gait. The problem was attributed to "tight heel cords," but casting was not effective. Achilles tendon lengthening greatly improved the patient's ability to walk. When pneumonia in the course of H1N1 influenza required hospitalization, a chest X-ray showed cardiomegaly. An echocardiogram detected a dilated left ventricle, hypertrophy of the left ventricular wall (LVW), and an ejection fraction of 44%. Heart function remained stable for 5 years, and yearly Holter monitoring revealed no episodes of arrhythmia. Initial genetic testing for FA identified a GAA expansion of 730 trinucleotide repeats and 1 normal allele. Shortly thereafter, however, the presence of a deletion (c.11_12TCdel) in 1 allele was identified. At the age of 8 years, the patient's mother noticed frequent urination, and a pediatrician diagnosed type 1 diabetes mellitus. Serum glucose levels rose to 500 mg/100 mL, but an insulin pump and glucose monitor achieved good diabetic control. At the age of

From the Research Service, Veterans Affairs Medical Center, Albany, New York (ABB, AHK); Department of Pathology, Albany Medical Center, Albany, New York (JQ, AHK); Department of Pathology and Laboratory Medicine, University of Texas Medical Branch, Galveston, Texas (BBG); Department of Pediatrics and Neurology, University of Colorado, Aurora, Colorado (MY); and Centogene, Rostock, Germany (PB).
Send correspondence to: Arnulf H. Koeppen, MD, Research Service (151), Veterans Affairs Medical Center, 113 Holland Avenue, Albany, NY 12208; E-mail: arnulf.koeppen@med.va.gov
Disclosure of funding: Friedreich's Ataxia Research Alliance to Arnulf H. Koeppen; National Institutes of Health, R01 NS06954 to Arnulf H. Koeppen; and Neurochemical Research, Inc. to Arnulf H. Koeppen.
Conflict of interest: The authors have no duality or conflicts of interest to declare.

9 years, the patient developed acute choreiform movements that were severe enough to interfere with his daily activities. His physicians diagnosed Sydenham chorea but antistreptococcal antibodies were not reactive. Divalproex sodium caused improvement for about 6 months, though the patient began using his wheelchair at all times. At the age of 11, he suddenly became apneic at night and had no pulse. Paramedics resuscitated him, and he was admitted to a local hospital. The reason for the sudden event was not established. He spent 1 week in a pediatric intensive care unit and was released home on hospice care. He died 3 months before his 12th birthday from heart failure. An autopsy was performed with specific attention to tissues affected by FA, and fixed and frozen samples were transferred to the research laboratory at the Veterans Affairs Medical Center (VAMC) in Albany, New York, for detailed morphologic and biochemical analyses. Extraction of DNA from the patient's frozen cerebellum and polymerase chain reaction (PCR) revealed 1 normal GAA repeat and one expanded allele (896). Blood samples were obtained from the parents, and analysis at Centogene, Rostock, Germany, revealed the deletion in the father's *FXN* and a GAA trinucleotide expansion of 952 in the mother. There were no other FA patients in the parents' extended families.

Compound Heterozygous FA Case 2, Man, 28. The patient's mother reported that her son did not grow properly at age 1–2 years in comparison with his older brother, but his physicians could not establish a cause. The diagnosis of FA was first made at the age of 6 years. At the age of 7–8 years, the patient used a walker, and at 9, required a wheelchair. At age 11, he underwent corrective surgery for scoliosis, and during the time of this hospitalization he developed diabetes mellitus. Several episodes of diabetic ketoacidosis occurred. At the age of 26 years, an episode of atrial flutter was the first indication of cardiomyopathy. Toward the end of his life, he developed visual failure, hearing deficit, and a neurogenic bladder. Despite severe disability, he graduated from high school. He died at 28 from an intracerebral hemorrhage. He had no genetic testing during his lifetime. PCR of his cerebellar DNA and gel electrophoresis confirmed 1 normal GAA repeat and one expanded allele (744). Sequencing of *FXN* at Centogene confirmed deletion of exon 5. Testing of the parents revealed the deletion in the father's DNA and a GAA trinucleotide repeat expansion of 862 in the mother. There were no other FA patients in the parents' extended families.

Homozygous FA Case 1, Boy, 10 (GAA 1016/1016). At the age of 2 years, the patient was hospitalized because of pneumonia. A chest X-ray revealed cardiomegaly. First neurologic symptoms and signs occurred at the age of 6, and the diagnosis of FA was established by genetic testing. Scoliosis became a problem, and at the age of 8, he developed insulin-dependent diabetes mellitus. In first grade, he began using a wheelchair, and according to his mother's account, his feet became "pointed". At the age of 10, he had Achilles tendon lengthening, but spasticity of the legs became troublesome. While admitted to a rehabilitation facility, an echocardiogram showed an apical thrombus, and enoxaparin was begun. The left ventricular ejection fraction was 27%. A transesophageal echocardiogram showed resolution of the apical thrombus but also a "rigid left ventricular wall". A computed tomogram of the brain detected a thalamic infarction, and MRI revealed additional ischemic lesions. Prolonged episodes of intense agitation were difficult to control and were later diagnosed as true seizures. The patient died at 10 years of age from liver and kidney failure. A brother and a sister have remained well.

Homozygous FA Case 2, Woman, 25 (GAA 800/1100). The patient's mother dated onset of FA in her daughter to age 4–5, and the onset of hypertrophic cardiomyopathy to age 5–6. At age 8, she needed support to walk and at 10 began to use a wheelchair full-time. She underwent placement of a Harrington rod at age 11 and developed insulin-dependent diabetes mellitus at age 13. The patient became totally disabled at age 22 and developed visual and hearing impairment. She died in a hospice setting at age 25 from heart failure. A brother, also affected by FA, preceded her in death at age 23. The parents' extended families do not include other FA cases.

MATERIALS AND METHODS

All procedures involving human participants were in accordance with the ethical standards implemented by the Institutional Review Board of VAMC Albany, New York. The inclusion of age-matched normal cases was intended to control for age-related differential vulnerability of heart and nervous tissue in FA.

Immunohistochemistry

Tissues relevant to FA were sampled, fixed, embedded in paraffin, and sectioned at 6-μm thickness to visualize selected proteins. Host, clonality, supplier, catalog number, antigen retrieval method, and final protein concentration of antibodies were as follows: N-cadherin, mouse monoclonal (IgG), Novus Biologicals, Littleton, CO, NBP1-48309, 0.01 M citric acid–sodium citrate buffer (pH 6) at 95 °C for 20 minutes, 2 μg/mL; S100, mouse monoclonal (IgG), Santa Cruz Biotechnology, Santa Cruz, CA, sc-53438, 0.01 M citric acid–sodium citrate buffer (pH 6) at 95 °C for 20 minutes, 0.8 μg/mL; myelin basic protein (MBP), mouse monoclonal (IgG), Covance, Emeryville, CA, SMI-94R, 80% ethanol extraction overnight at 4 °C, ascites fluid (protein not assayed); phosphorylated neurofilament protein, mouse monoclonal (IgG), Sternberger Monoclonals, Inc., Lutherville, MD (now Covance), SMI-31R, 0.01 M citric acid–sodium citrate buffer (pH 6) at 95 °C for 20 minutes, ascites fluid (protein not assayed); glial fibrillary acidic protein (GFAP), mouse monoclonal (IgG), Covance, SMI-21R, 1× solution (vol/vol) of DIVA, a proprietary antigen retrieval mixture (Biocare Medical, Concord, CA; DV2004) at 95 °C for 30 minutes, ascites fluid (protein not assayed); laminin, mouse monoclonal (IgG), Sigma Aldrich, St. Louis, MO, L8271, proteinase K digestion at 37 °C for 30 minutes, ascites fluid (protein not assayed); neuron-specific enolase (NSE), mouse monoclonal (IgG), Millipore, Billerica, MA, MAB324, DIVA, 10 μg/mL; glutamic acid decarboxylase (GAD), mouse monoclonal (IgG), MBL International, Woburn, MA, M018-3, DIVA, 4 μg/mL.

A summary of the immunohistochemical procedure is available from references (5–7).

Selected samples of dorsal roots (DR) were also embedded in resin by standard methods. Semi-thin sections of 1-μm thickness were cut on a Leica Ultracut S ultramicrotome and stained with Toluidine Blue (University of Texas Medical Branch, Galveston, TX).

Enzyme-Linked Immunosorbent Assay (ELISA) of Frataxin

Frataxin levels were assayed in extracts of frozen LVW and dentate nuclei (DN) from the 4 FA patients, and 6 normal controls (for LVW, ages 36–74; for DN, ages 51–85) as described previously (5, 6). Tissue frataxin concentrations were expressed as nanograms per gram original wet weight.

RESULTS

Autopsy Findings

Compound Heterozygous FA Case 1, Boy, 11. The weights of heart and brain were 288 and 1148 g, respectively. The heart showed concentric hypertrophy. Sections revealed cardiomyocyte hypertrophy and extensive endomysial fibrosis. The pancreas showed few islets, and most contained only 2–4 synaptophysin-reactive β-cells. Sections of the cerebrum revealed the absence of Betz cells, hypoxic neuronal changes, astrogliosis, microglial proliferation in the pyramidal layer of the hippocampus, multiple small infarctions in the left striatum, and diffuse gliosis of the thalamus. The substantia nigra revealed hypoxic nerve cell changes. The cerebellar cortex showed regional loss of Purkinje cells, empty baskets, and scattered torpedoes. The DN revealed severe neuronal loss. At the level of the medulla oblongata, gracile and cuneate nuclei displayed no convincing loss of nerve cells. Hypercellularity and small neuronal sizes in DR ganglia (DRG), long-tract fiber degeneration of the spinal cord, and lack of neurons in the dorsal nuclei were consistent with FA.

Compound Heterozygous FA Case 2, Man, 28. The weights of heart and brain were 439 and 1120 g, respectively. The heart showed concentric hypertrophy, but the mural thrombus had resolved. Sections confirmed cardiomyocyte enlargement and a moderate increase of endomysial connective tissue. A synaptophysin stain of the pancreas revealed very few islets. The motor cortex was devoid of Betz cells. A small cortical infarction was present. In the medulla oblongata, gracile and cuneate nuclei were normal. The cerebellar cortex was

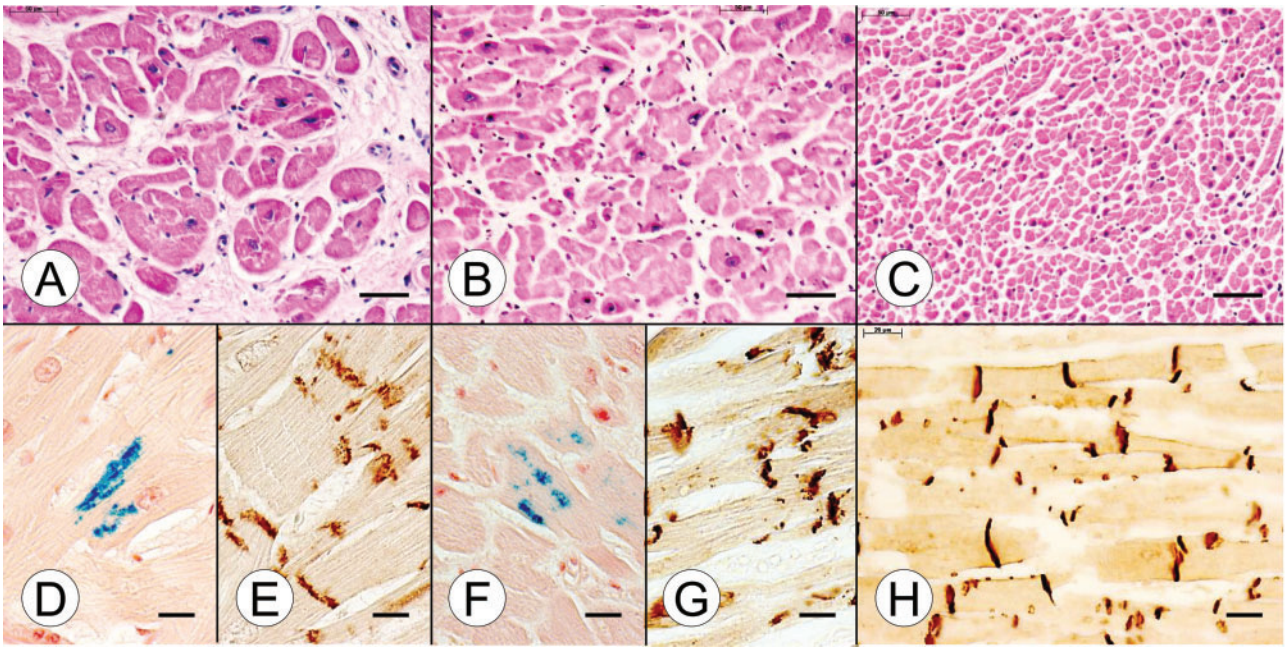

FIGURE 1. Cardiac pathology in juvenile compound heterozygous and homozygous Friedreich ataxia (FA). (**A**, **D**, **E**) Compound heterozygous FA case 1; boy, 11; (**B**, **F**, **G**) homozygous FA case 1; boy, 10; (**C**, **H**) normal control; boy, 9. (**A**) The cross section of the ventricular septum (VS) in the compound heterozygote shows cardiomyocyte enlargement, excessive lobulation of fibers, and endomysial fibrosis. **(B)** The comparable section of VS in the homozygous FA patient is similar though endomysial fibrosis is less prominent. **(C)** The section of the VS from an age-matched control reveals the great abundance of small normal cardiomyocytes and a delicate endomysium. **(D, F)** Longitudinal sections of the VS in the compound heterozygous FA case 1 **(D)** and the age-matched homozygous FA case 1 **(F)** reveal iron-containing inclusions. **(E, G)** N-cadherin immunohistochemistry shows large disrupted intercalated discs (ICD) in both the compound heterozygous FA case 1 **(E)** and the age-matched homozygous FA case 1 **(G)**. **(H)** N-cadherin immunohistochemistry of the normal VS shows small ICD that are aligned in register across adjacent heart fibers. The ICD also display a lesser degree of undulation than in FA **(E, G)**. **(A–C)** Hematoxylin and eosin; **(D, F)** Perls's stain for iron; **(E, G, H)** immunohistochemistry for N-cadherin. Scale bars: **(A–C)**, 50 μm; **(D–H)**, 20 μm.

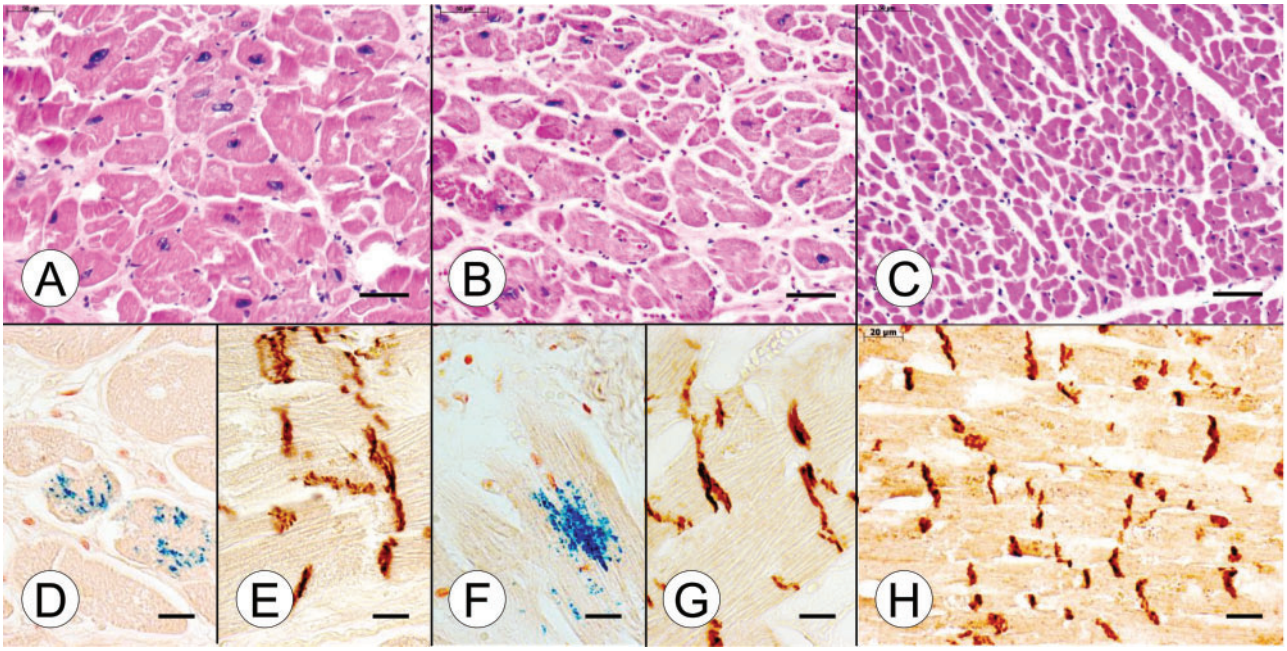

FIGURE 2. Cardiac pathology in adult compound heterozygous and homozygous Friedreich ataxia (FA). (**A**, **D**, **E**) Compound heterozygous FA case 2; man, 28; (**B**, **F**, **G**) homozygous FA case 2; woman, 25; (**C**, **H**) normal control; man, 41. **(A**, **B)** Cross-sections of the ventricular septum (VS) show comparable cardiomyocyte hypertrophy in the adult compound heterozygous **(A)** and the homozygous FA **(B)** cases. **(C)** The cross-sectional areas of normal cardiomyocytes are much smaller than in FA. **(D**, **F)** Iron histochemistry of the VS in adult compound heterozygous **(D)** and adult homozygous FA **(F)** generates finely granular blue reaction product in cardiomyocytes. (**E**, **G**) N-cadherin reaction product shows large disorganized intercalated discs (ICD) in adult compound heterozygous FA (**E**) and adult homozygous FA (**G**). **(H)** N-cadherin reaction product in normal myocardium shows tight, small ICD that are aligned in register across adjacent fibers. **(A–C)** Hematoxylin and eosin; **(D**, **F)** Perls's stain for iron; **(E**, **G**, **H)** immunohistochemistry for N-cadherin. Scale bars: **(A–C)**, 50 μm; **(D–H)** 20 μm.

normal, but the DN displayed subtotal loss of neurons. DRG and spinal cord were consistent with FA.

A systematic side-by-side comparison of cardiac and nervous system pathology of the compound heterozygous and homozygous FA cases, and normal controls, appears in Figures 1–8. A section of the myocardium (ventricular septum [VS]) in the young compound heterozygote FA case 1 shows cardiomyocyte hypertrophy and endomysial fibrosis (Fig. 1A), iron-reactive inclusions in heart fibers (Fig. 1D), and disruption of intercalated discs (ICD) (Fig. 1E). The cardiac lesion in the young homozygous FA case 1 is very similar (Fig. 1B, F, G). The VS of a normal control case of comparably young age (9 years) shows a great abundance of small heart fibers (Fig. 1C), thin endomysium, and regular alignment of ICD (Fig. 1H). Iron stains revealed no reactive inclusions (not illustrated). In the VS of the adult compound heterozygous FA case 2 (Fig. 2A) and the age-matched homozygous FA case 2 (Fig. 2B), the lesion is very similar to that of the young FA patients (Fig. 1). Figure 2C illustrates the dramatic difference in cardiomyocyte size between a normal control and the FA patients (Fig. 2A, B). Iron-reactive inclusions are present in the VS of the adult compound heterozygous FA case 2 (Fig. 2D) and the homozygous FA case 2 (Fig. 2F). ICD in the adult FA patients are abnormally large and irregular (Fig. 2E, G). In the normal control, ICD are much smaller and display their regular alignment across adjacent fibers (Fig. 2H).

Abnormalities in the DRG in the young compound heterozygous and homozygous FA patients (Fig. 3A and B, respectively) are very similar, consisting of hypercellularity, residual nodules (Fig. 3A and B, arrows), and overall smaller neuronal size compared with a 9-year-old normal control (Fig. 3C). Satellite cells with S100-immunoreactivity appear less abundant in the compound heterozygous FA case 1 (Fig. 3D) than in the homozygous FA case 1 (Fig. 3E), but the former case shows reaction product in residual nodules (Fig. 3D, arrow). In the normal control, S100-positive satellite cells form a single layer around DRG neurons (Fig. 3F). A stain for MBP shows similar depletion of myelinated fibers in the dorsal columns of the thoracic spinal cord in the compound heterozygous and homozygous FA patients (Fig. 3G and H, respectively). Loss of fibers in the dorsal spinocerebellar and lateral corticospinal tracts is less convincing in the compound heterozygote (Fig. 3G) than in the homozygote (Fig. 3H). Neurons in the dorsal nuclei are absent in both FA cases (Fig. 3G and H, insets). The larger cross-sectional area of the thoracic spinal cord in the normal control is very evident (Fig. 3I), as is the bulge of the dorsal nucleus (Fig. 3I, arrow). The normal specimen also shows the large diameter (~50 μm) of a neuron in the dorsal nucleus (Fig. 3I, inset). In the adult cases of compound heterozygous and homozygous FA, the difference in the size of DRG neurons (Fig. 4A, B) is more apparent than in the juvenile cases of the disease (Fig. 3A, B). Stains for S100 confirm the size differences between the

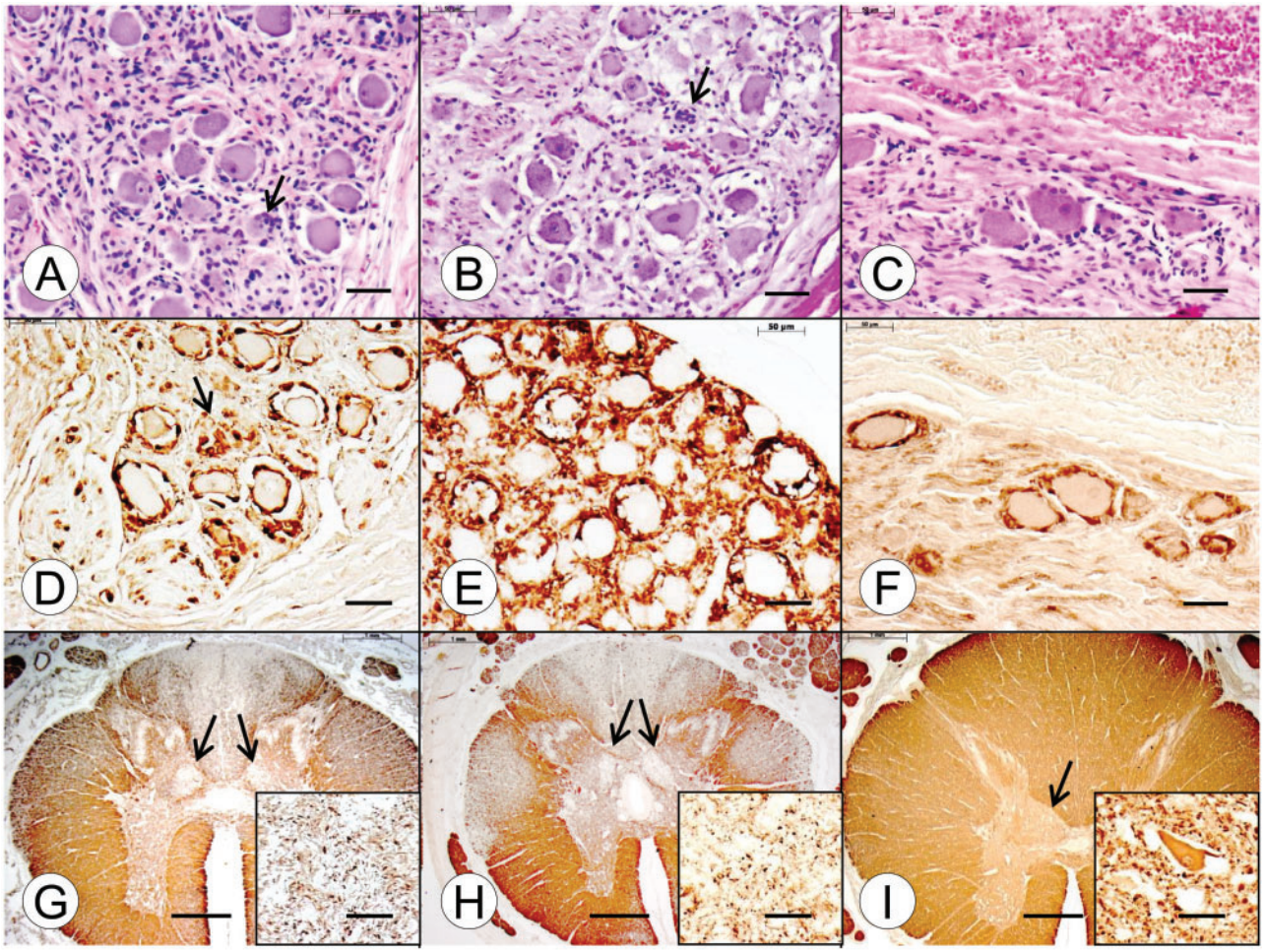

FIGURE 3. Dorsal root ganglia (DRG) and thoracic spinal cord in juvenile compound heterozygous and homozygous Friedreich ataxia (FA). **(A**, **D**, **G)** Compound heterozygous FA case 1; boy, 11; **(B**, **E**, **H)** homozygous FA case 1; boy, 10; **(C**, **F**, **I)** normal control; boy, 9. (**A**–**C**) DRG in the compound heterozygous **(A)** and homozygous FA **(B)** cases show hypercellularity and residual nodules (arrows). The overall neuronal size in the FA cases is smaller than normal **(C)**. **(D–F)** Prominent S100 reaction product is present in satellite cells of the DRG in the compound heterozygous FA case 1 **(D)** and homozygous FA case 1 **(E)**. The arrow in **(D)** indicates an S100-reactive residual nodule. In the case of homozygous FA **(E)**, S100 immunohistochemistry suggests an abnormal abundance of satellite cells, compared to the normal control **(F)**. **(G–I)** The cross-sectional area of the thoracic spinal cord in compound heterozygous **(G)** and homozygous FA **(H)** is smaller than normal **(I)**. In the compound heterozygous FA case **(G)** and the homozygous FA case **(H)**, depletion of myelinated fibers in the dorsal columns is comparable. Fiber loss in the dorsal spinocerebellar and lateral corticospinal tracts of the compound heterozygote **(G)** is less prominent than in the homozygous case **(H)**. The myelin basic protein (MBP) stains also show fiber depletion in the dorsal nuclei in compound heterozygous FA (**G,** arrows) and homozygous FA (**H,** arrows). In the normal spinal cord, the dorsal nucleus is distinctly visible (**I,** arrow). **(G–I**, insets**)** Immunohistochemistry for class-III-β-tubulin reveals total loss of large neurons in the compound heterozygous **(G**, inset**)** and homozygous **(H**, inset**)** FA cases. The class-III-β-tubulin stain in the normal control **(I**, inset**)** reveals a large normal neuron with a maximum diameter of approximately 50 μm. **(A–C)** Hematoxylin and eosin; **(D–F)** immunohistochemistry for S100; **(G–I)** immunohistochemistry for MBP; **(G–I**, insets**)** immunohistochemistry for class-III-β-tubulin. Scale bars: **(A–F)**, 50 μm; **(G–I)**, 1 mm; **(G–I**, insets**)**, 50 μm.

neuronal voids in the FA cases (Fig. 4D, E) and the normal control (Fig. 4F). Residual nodules are immunoreactive with anti-S100 (Fig. 4D and E, arrows). In these adult compound heterozygous and homozygous FA cases, depletion of myelinated fibers in dorsal columns, dorsal spinocerebellar tracts, and lateral corticospinal tracts are well established (Fig. 4G, H), as is the lack of neurons in the dorsal nuclei (Fig. 4G and H, insets). The cross-sectional area of the normal spinal cord (Fig. 4I) is larger than that in FA (Fig. 4G, H), and the dorsal nucleus displays a large nerve cell (diameter of >50 μm [Fig. 4I, inset]).

Figures 5A–L and 6A–M present a comparison of the DR in the juvenile compound heterozygous FA case 1, the adult compound heterozygous FA case 2, and the age-matched homozygous FA cases. In 3 of 4 FA cases. DR show peculiar balloon-like expansions that displace axons

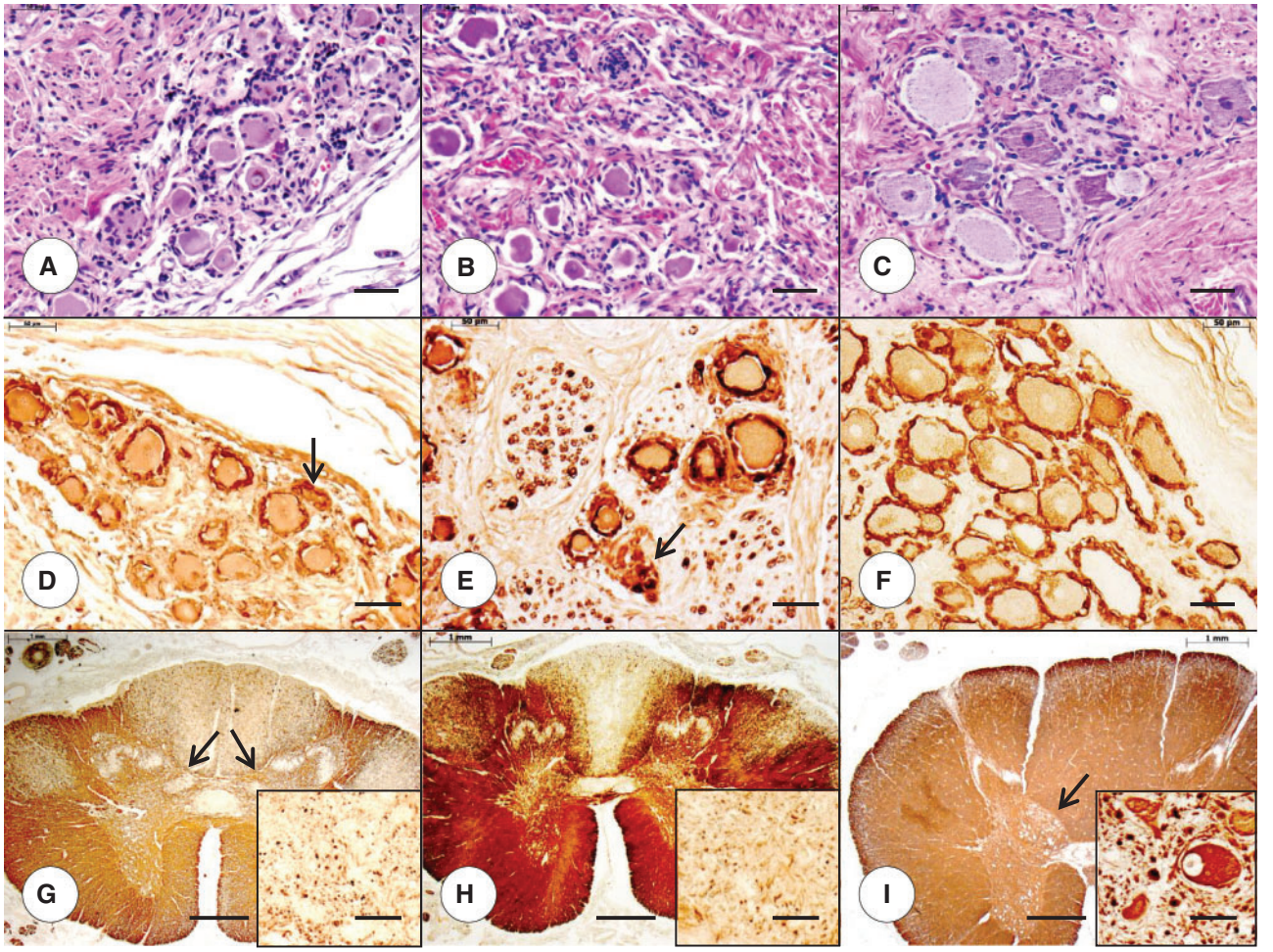

FIGURE 4. Dorsal root ganglia (DRG) and thoracic spinal cord in adult compound heterozygous and homozygous Friedreich ataxia (FA). **(A**, **D**, **G)** Compound heterozygous FA case 2; man, 28; **(B**, **E**, **H)** homozygous FA case 2; woman, 25; (**C**, **F**, **I)** normal control; man, 48. **(A–C)** DRG neurons in the compound heterozygous FA case 2 **(A)** and homozygous FA case 2 **(B)** are noticeably smaller than the nerve cells in the normal control **(C)**. **(D–F)** S100 immunohistochemistry reveals reaction product in residual nodules in compound heterozygous FA (**D**, arrow) and homozygous FA (**E**, arrow) and generates smaller negative images of neurons in FA **(D**, **E)** than in the control **(F)**. **(G–I)** MBP immunohistochemistry shows comparable fiber depletion in the compound heterozygous FA case 2 **(G)** and the homozygous case 2 **(H)**. The cross-sectional area of the thoracic spinal cord in compound heterozygous (**G)** and homozygous FA **(H)** is smaller than normal **(I)**. The MBP stain of the cord in compound heterozygous FA also reveals a diminutive bulge of the dorsal nuclei (**G,** arrows). (**G–I**, insets) Class-III-β-tubulin immunohistochemistry confirms the total lack of large neurons in dorsal nuclei in the compound heterozygous FA (**G,** inset) and homozygous FA (**H,** inset). The normal control shows a typical elliptical nerve cell with a peripherally placed nucleus (**I**, inset). **(A–C)** Hematoxylin and eosin; **(D–F)** immunohistochemistry for S100; **(G–I)** immunohistochemistry for MBP; **(G–I**, insets**)** immunohistochemistry for class-III-β-tubulin. Scale bars: **(A–F)**, 50 μm; **(G–I),** 1 mm; **(G–I**, insets**)**, 50 μm.

(Figs. 5A, B, 6A), differing greatly from the regularly arranged large and small fibers in the normal control (Figs. 5C, 6D). The expansions are reactive with antibodies to S100 (Figs. 5D, F, 6E) and GFAP (Figs. 5E, G, 6F). Of note, the overall abundance of S100 reaction product in the DR of the FA cases is reduced, implying a paucity of Schwann cell cytoplasm. In contrast, the normal juvenile control reveals an organized ensheathment of large and small axons in DR (Fig. 5H), and a lack of GFAP expression (Fig. 5I). The expansions are not immunoreactive with an antibody to laminin, but are surrounded by a thin layer of reaction product (Fig. 5J, K). This thin membrane is also apparent on a resin-embedded section (Fig. 5K, inset, arrow). Between the expansions, the DR parenchyma displays intense laminin reactivity that surrounds thin myelinated and nonmyelinated axons (Fig. 5J, K). The cross-section of a normal DR reveals a regular honeycomb-like pattern of reaction product (Fig. 5L). The DR of the adult compound heterozygous FA case 2 and the homozygous FA case 2 show a dearth of large axons (Fig. 6A–C) when compared with a normal control (Fig. 6D). In some DR of the compound heterozygous FA case 2, S100- and GFAP-immunoreactive expansions (Fig. 6E and F, respectively) are identical to those of the juvenile FA cases (Fig. 5). Similar to the juvenile cases, S100-reactive Schwann cells in DR of adult

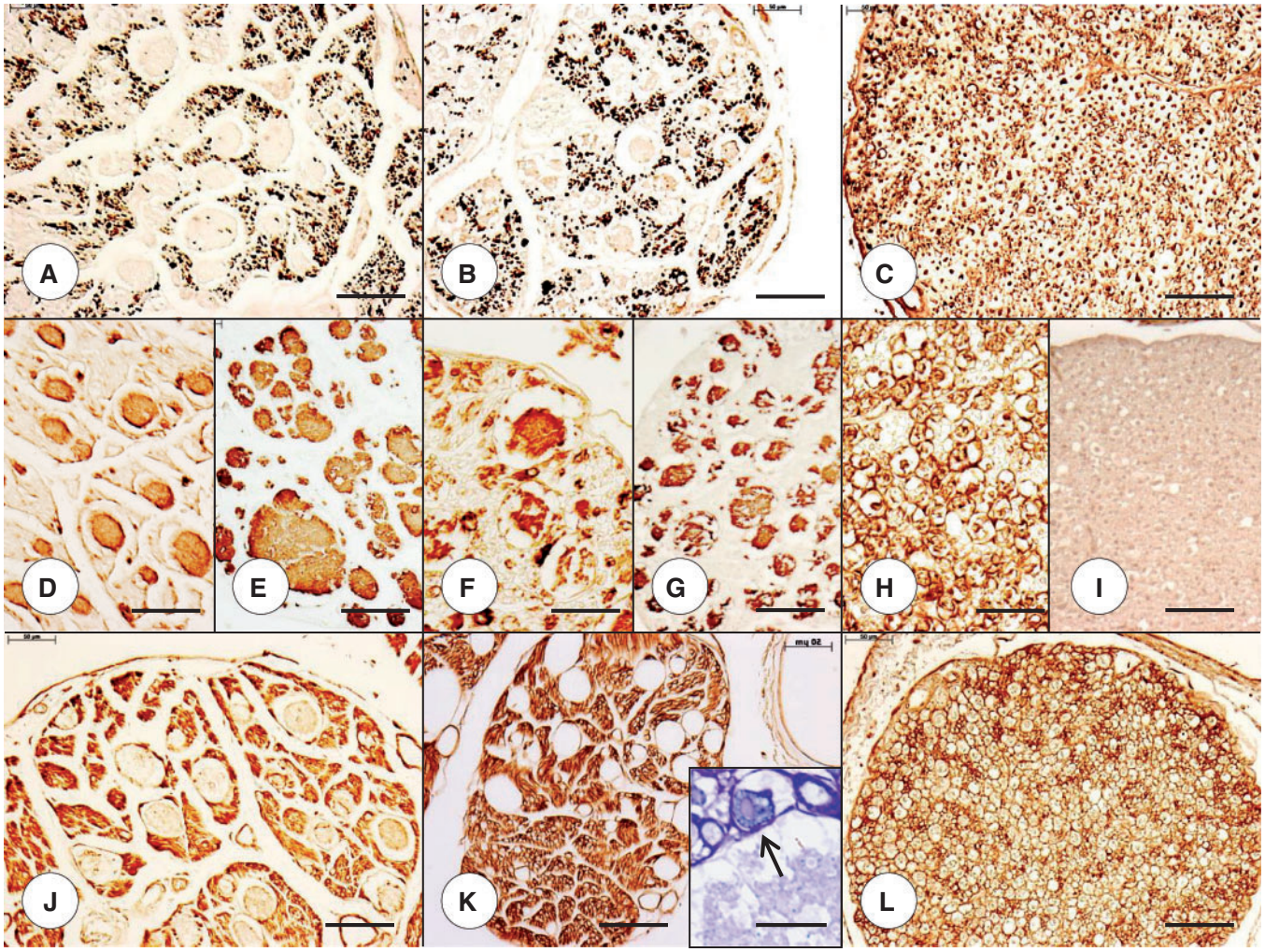

FIGURE 5. Dorsal roots (DR) in juvenile compound heterozygous and homozygous Friedreich ataxia (FA). **(A, D, E, J)** Compound heterozygous FA case 1; boy 11; **(B, F, G, K)** homozygous FA case 1; boy 10; **(C, H, I, L)** normal control; boy, 9. **(A–C)** The axon stain shows negative images of expansions within the substance of the DR in compound heterozygous case 1 **(A)** and homozygous FA case 1 **(B)**. The organized distribution of large and small axons of the normal DR is absent **(C)**. **(D–I)** The expansions in the DR yield reaction product with anti-S100 in compound heterozygous FA case 1 **(D)** and homozygous FA case 1 **(F)**. The glial fibrillary acidic protein (GFAP) stain yields similar results **(E, G)**. In the normal control case **(H, I)**, S100 reaction product shows delicate rims around large and small DR axons **(H)** but no GFAP **(I)**. The DR in compound heterozygous FA **(D)** and homozygous FA **(F)** show a deficit of S100 in regions occupied by axons **(A, B)**. **(J–L)** The expansions in DR are negative for laminin but are surrounded by a delicate layer of reaction product in compound heterozygous FA **(J)** and homozygous FA **(K)**. The normal DR **(L)** reveal a honeycomb-like pattern of laminin reaction product around large axon and islands of small axons. This pattern is absent from the DR in compound heterozygous FA **(J)** and homozygous FA **(K)**. **(A-C)** Immunohistochemistry for phosphorylated neurofilament protein; **(D, F, H)** immunohistochemistry for S100; **(E, G, I)** immunohistochemistry for GFAP; **(J–L)** immunohistochemistry for laminin; **(K**, inset**)** resin-embedded section stained with Toluidine blue. Scale bars: **(A–L),** 50 μm; **(K**, inset**),** 20 μm.

FA cases (Fig. 6E, G) are sparse in comparison with the great abundance in the control case (Fig. 6I). The DR of homozygous FA case 2 (Fig. 6H) and the normal control (Fig. 6J) are GFAP-negative. In the control case, GFAP immunoreactivity ends at the DR entry zone (Fig. 6J, inset, arrow). An antibody to laminin reveals compact reaction product surrounding thin fibers in the DR of both compound heterozygous (Fig. 6K) and homozygous FA cases (Fig. 6L). The DR of a normal adult control shows delicate circles of laminin reaction product, yielding a regular honeycomb-like pattern (Fig. 6M and inset).

Figures 7 and 8 display the lesion of the DN in compound heterozygous and homozygous FA. All FA cases show loss of nerve cells (Figs. 7A, B, 8A, B) and GAD-reactive terminals (Figs. 7D, E, 8D, E). Grumose regeneration is present in the young compound heterozygous case 1 (Fig. 7D, inset).

Frataxin levels in the LVW and DN in the FA cases were at or below the detection limits of ELISA (10 pg or ≤10 ng/g wet weight). In the LVW of 6 normal controls, the frataxin levels were 266 ± 92 ng/g wet weight (mean ± SD).

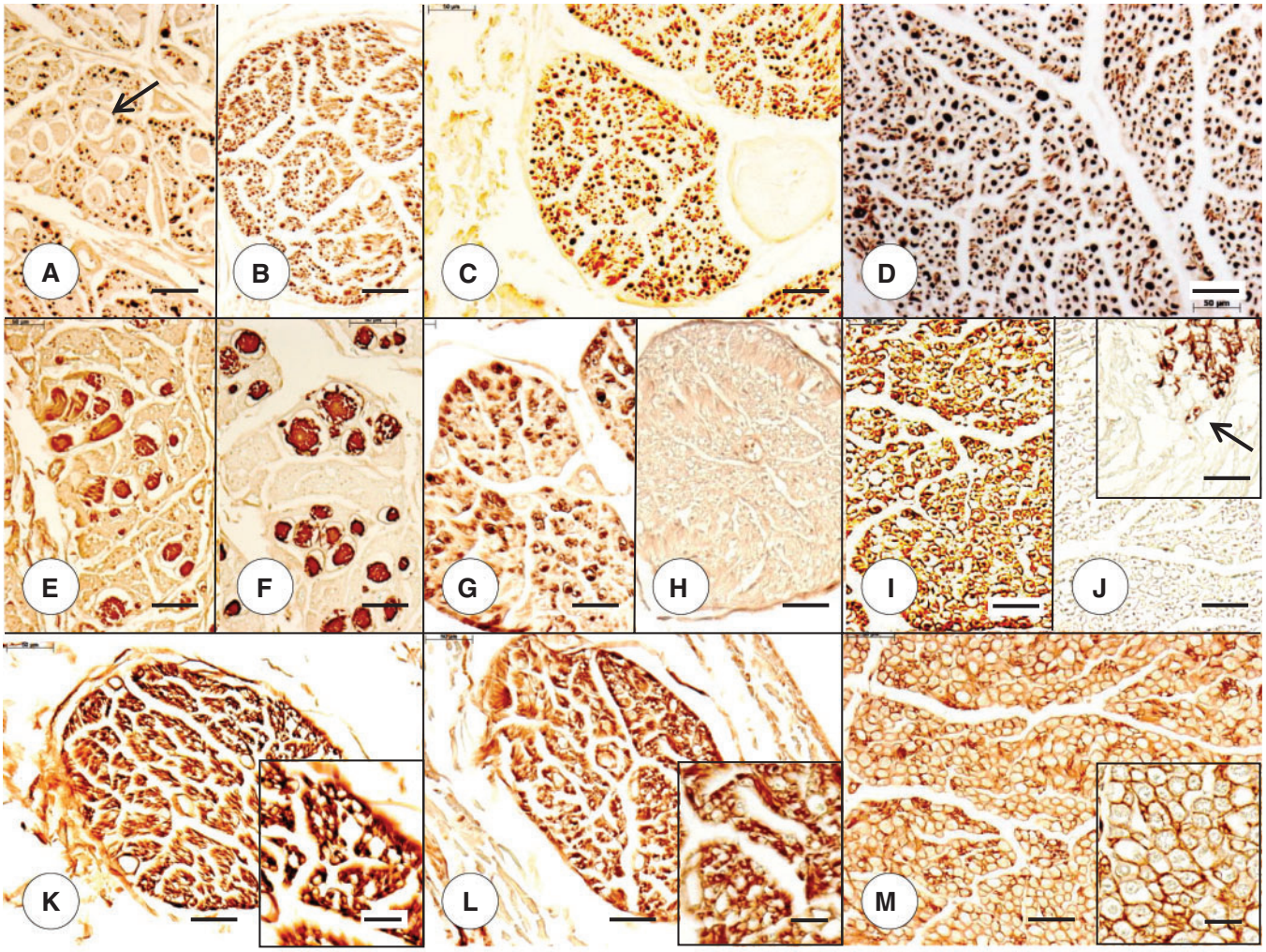

FIGURE 6. Dorsal roots (DR) in adult compound heterozygous and homozygous Friedreich ataxia (FA). **(A**, **B**, **E**, **F**, **K)** Compound heterozygous FA case 2; man, 28; **(C**, **G**, **H**, **L)** homozygous FA case 2; woman, 25; **(D**, **I**, **J**, **M)** normal control; woman, 38. **(A**–**D)** The DR of the compound heterozygous **(B)** and the homozygous **(C)** FA cases indicate a relative lack of large axons. In some DR of the compound heterozygous FA case 2 (**A,** arrow), the stain reveals similar expansions as illustrated in Figures 5A and B. **(E**–**J)** The DR expansions in the compound heterozygous case are reactive with antibodies to S100 **(E)** and glial fibrillary acidic protein (GFAP) **(F)**. DR in the homozygous FA case show a deficit in S100 reaction product **(G)** but are GFAP-negative **(H)**. The normal DR in the control specimen displays more abundant S100 reaction product **(I)** and is GFAP-negative **(J)**. GFAP immunoreactivity attributable to the central nervous system ends at the DR entry zone (**J,** inset, arrow). **(K**–**M)** The DR of the compound heterozygous FA case 2 **(K)** and the homozygous FA case 2 **(L)** show compact laminin reaction product around the voids of thin axons (**K**, **L,** insets). The normal DR **(M)** displays the orderly honeycomb-like reaction product of laminin (**M** and **M**, inset). **(A**–**D)** Immunohistochemistry for phosphorylated neurofilament protein; **(E**, **G**, **I)** immunohistochemistry for S100; **(F**, **H**, **J)** immunohistochemistry for GFAP; **(K**–**M** and insets**)** immunohistochemistry for laminin. Scale bars: **(A**–**M),** 50 μm; **(J**–**M**, insets**)**, 20 μm.

In the DN of 6 normal controls, frataxin levels were 126 ± 43 ng/g wet weight (mean ± SD).

DISCUSSION

Comparison of Clinical Features

Early age of onset, cardiomyopathy, and insulin-dependent diabetes mellitus were similar in the described cases of compound heterozygous and age-matched homozygous FA patients. Of note, homozygous FA patient 1 had spastic legs, perhaps reflected by the more prominent fiber loss in the lateral corticospinal tracts (Fig. 3H). Chorea is an unusual manifestation of FA (8–10). Spacey et al reported chorea in one of 2 compound heterozygous siblings with FA who had the same deletion as compound heterozygous FA case 1, c.11_12TCdel, in 1 allele (9). Chorea was present at the time of first neurologic examination in all previously reported cases. This hyperkinetic movement disorder, however, is not unique to compound heterozygous FA, as Zhu et al described 1 FA patient with GAA expansions on both alleles

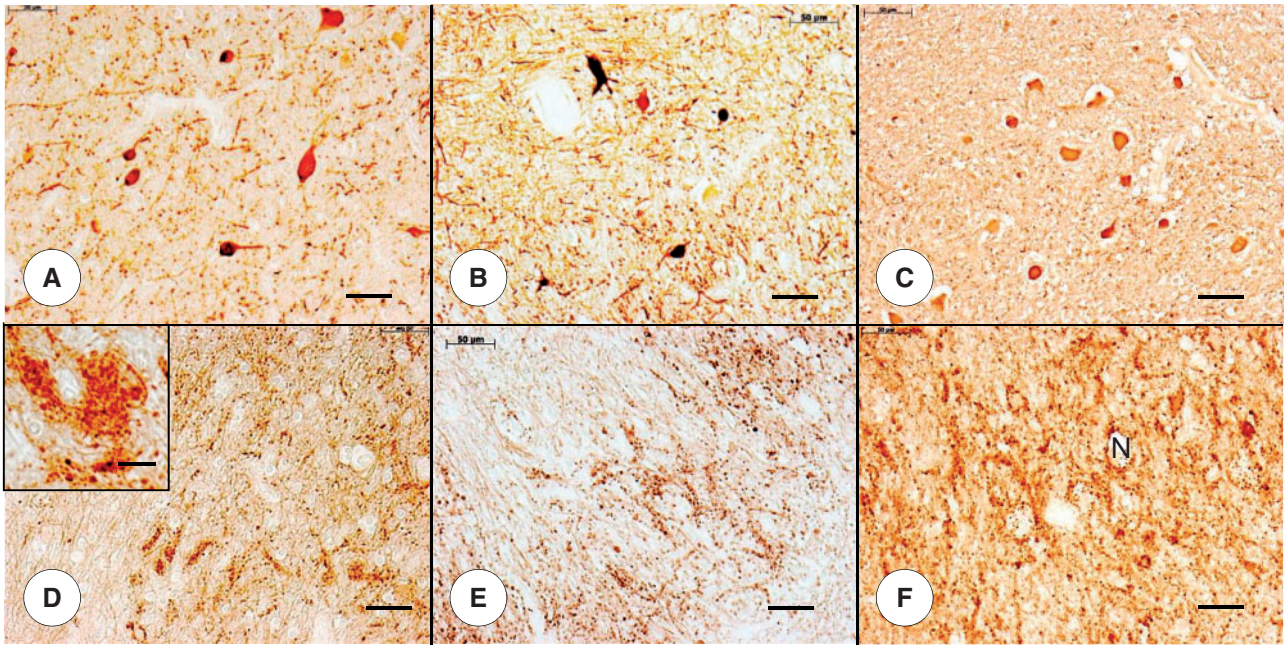

FIGURE 7. Dentate nucleus (DN) in juvenile compound heterozygous and homozygous Friedreich ataxia (FA). **(A, D)** Compound heterozygous FA case 1; boy 11; **(B, E)** homozygous FA case 1; boy 10; **(C, F)** normal control; boy, 9. **(A–C)** The DN of the compound heterozygous **(A)** and homozygous **(B)** FA cases show neuronal loss. In this age group, the distinction between large and small DN neurons in the normal control is not yet evident **(C)**. **(D–F)** glutamic acid decarboxylase (GAD) immunohistochemistry shows a lack of GABA-ergic terminals in the DN in the compound heterozygous FA case **(D)** that is comparable to the homozygous FA case **(E)**. The inset in **(D)** displays grumose regeneration in compound heterozygous FA. In the normal control **(F)**, GAD reaction product is very abundant and generates neuronal voids ("N"). **(A–C)** Immunohistochemistry for NSE; **(D–F)** immunohistochemistry for GAD. Scale bars: 50 μm.

who also had chorea (10). One previously reported heterozygous FA patient had dystonia (4). The pathogenic variants reported here may be classified as "null" mutations (2), and clinical manifestations are expected to correlate with frataxin levels arising from transcription of the expanded allele. Galea et al determined that the prevalence of cardiomyopathy is higher in homozygous than in compound heterozygous FA patients, which is at variance with the observations reported here (2). A logical explanation for the similar clinical phenotype in compound heterozygous FA case 1 and homozygous FA case 1 is shared severe frataxin deficiency. Neither patient had frataxin assays in blood, lymphocytes, or buccal cells, but frataxin levels in 2 tissues that are primary targets of FA, namely, heart and DN, were at or below the detection limits of ELISA.

Comparison of the Cardiac and Neuropathologic Phenotypes

The pathologic phenotypes of heart, DRG, spinal cord, DR, and DN did not reveal major differences between compound FA heterozygosity and FA homozygosity. We believe that the balloon-like swellings in DR expressing S100 and GFAP in both compound heterozygous FA cases and homozygous FA case 1 (Figs. 5D–G, 6E, F) represent an abnormal extension of spinal cord tissue across the DR entry zone. It appears less likely that they derive from nonmyelinating Schwann cells. A widely recognized abnormality in DR of FA is an abundance of thin axons and lack of large myelinated fibers (11). FA lesions affecting DRG and DR should also be interpreted as the result of frataxin deficiency in the neural crest during development (review in Ref. 12), causing incomplete demarcation of central and peripheral nervous systems in DR entry zones.

All FA cases showed depletion of GABA-ergic terminals in the DN. Grumose reaction in the DN, a peculiar proliferation of GAD-positive synaptic terminals (Fig. 7D, inset), is present in most but not all cases of FA. Grumose reaction disappears in cases of long duration, and Koeppen et al suggested that superimposed Purkinje cell atrophy is responsible for the ultimate loss of the GAD-reactive terminals in the DN (5).

The pathologic substrate of chorea in the previously published cases (8–10) is uncertain, and these reports did not include MRI. In the present compound heterozygous FA case 1, the striatum showed multiple small infarctions that were more recent than the onset of chorea at age 9. Also, widespread gliosis was more likely the result of recent hypoxia than frataxin deficiency.

Tissue samples available from the adult homozygous FA case 2 included a sural nerve specimen. Sections showed severe reduction in the number of large myelinated fibers while thin axons were abundant. Quantitative findings in this and other FA cases were previously published from this laboratory (13). Though sensory neuropathy was present by electrodiagnostic criteria in the juvenile compound heterozygous FA case 1, we could not make a systematic comparison

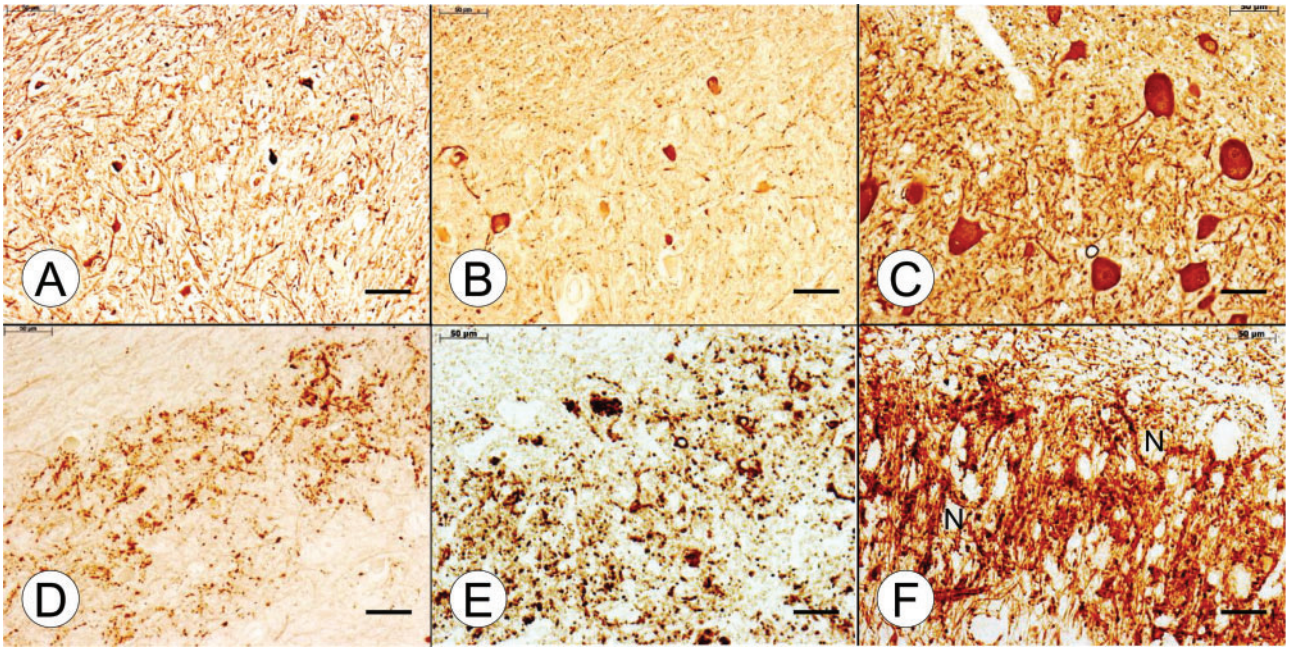

FIGURE 8. Dentate nucleus (DN) in adult compound heterozygous and homozygous Friedreich ataxia (FA). **(A, D)** Compound heterozygous FA case 2; man, 28; **(B, E)** homozygous FA case 2; woman, 25; **(C, F)** normal control; woman, 50. **(A–C)** The DN in compound heterozygous FA case 2 **(A)** and homozygous FA case 2 **(B)** show a comparable loss of large neurons. Only a few small NSE-reactive nerve cells remain. The normal adult DN **(C)** displays numerous large and interspersed small neurons, and elaborate dendrites. In this age group, size differences in DN neurons are distinct **(C)**. **(D–F)** Comparable loss and disorganization of GABA-ergic terminals are visible by glutamic acid decarboxylase (GAD) immunohistochemistry of the DN in compound heterozygous FA case 2 **(D)** and homozygous FA case 2 **(E)**. In the normal DN **(F)**, GAD reaction product shows a great abundance of terminals and generates negative images of neurons ("N"). **(A–C)** Immunohistochemistry for NSE; **(D–F)** immunohistochemistry for GAD. Scale bars: 50 μm.

of sural nerves in homozygous and compound heterozygous age-matched FA cases.

Frataxin Deficiency as the Common Denominator in the Pathogenesis of FA

In a comprehensive analysis of 111 FA patients harboring 63 different point mutations, insertions, or deletions in 1 allele and GAA expansions in the other, the impact on clinical features ranged from minimal to moderate or strong (2). The deletion in one allele of the *FXN* gene reported here (compound heterozygous FA case 1) probably caused a truncated, functionally deficient protein. In this and other "null" mutations, transcription of the expanded allele may be expected to generate normal frataxin, though at an insufficient amount (2, 4). The deletion of exon 5 in the compound heterozygous FA case 2 is similar to that in a previously reported heterozygous FA patient (14). This patient, a 21-year-old woman, had 820 GAA trinucleotide repeats and deletion of exon 5a. Symptoms and signs were characteristic of juvenile onset FA (age 9) and included cardiomyopathy and wheelchair use at age 15. Frataxin levels in peripheral tissues were not assayed, but it is likely that transcription of the allele with the deletion caused a truncated protein. In the autopsy tissues assayed in our study, subtotal deficiency of frataxin was present in both heterozygous cases. Hypertrophic cardiomyopathy, diabetes mellitus, the neural lesions, and severe frataxin deficiency were similar to those expected in homozygous FA patients with long GAA repeats in the shorter allele of the *FXN* gene (15).

The clinical and pathologic phenotypes in the 2 compound heterozygous FA cases reported here are not representative of all patients with 1 GAA expansion and point mutations, deletions, or insertions in the second allele. The impact of these mutations depends on the biosynthesis of tissue frataxin. Levels of this critically important mitochondrial protein in readily accessible tissue samples, such as lymphocytes or buccal cells, may serve as surrogate markers for frataxin deficiency in vulnerable tissues, such as heart, pancreas, DN, and DRG.

ACKNOWLEDGMENTS

The authors thank the families of the 4 FA patients for allowing autopsies to advance research in Friedreich ataxia. Dr. Ed Grabczyk, Louisiana State University Health Sciences Center, New Orleans, Louisiana, confirmed the GAA trinucleotide repeat expansion in compound heterozygous case 1 and the patient's mother by Southern blotting. The described work was completed in the laboratories of the Veterans

Affairs Medical Center, Albany, New York, and University of Texas Medical Branch, Galveston, Texas.

REFERENCES

1. Delatycki MB, Williamson R, Forrest SM. Friedreich ataxia: an overview. J Med Genet 2000; 37:1–8
2. Galea CA, Huq A, Lockhart PJ, et al. Compound heterozygous FXN mutations and clinical outcome in Friedreich ataxia. Ann Neurol 2016; 79: 485–95
3. Cossée M, Dürr A, Schmitt M, et al. Friedreich's ataxia: point mutations and clinical presentation of compound heterozygotes. Ann Neurol 1999; 45:200–6
4. De Castro M, Garcia-Planells J, Monrós E, et al. Genotype and phenotype analysis of Friedreich's ataxia compound heterozygous patients. Hum Genet 2000;106:86–92
5. Koeppen AH, Ramirez RL, Becker AB, et al. Friedreich ataxia: failure of GABA-ergic and glycinergic synaptic transmission in the dentate nucleus. J Neuropathol Exp Neurol 2015;74:166–76
6. Koeppen AH, Ramirez RL, Becker AB, et al. The pathogenesis of cardiomyopathy in Friedreich ataxia. PLoS One 2015;10:e0116396
7. Koeppen AH, Ramirez RL, Becker AB, et al. Dorsal root ganglia in Friedreich ataxia: satellite cell proliferation and inflammation. Acta Neuropathol Commun 2016;4:46
8. Hanna MG, Davis MB, Sweeney MG, et al. Generalized chorea in two patients harboring the Friedreich's ataxia gene trinucleotide repeat expansion. Mov Disord 1998;13:339–40
9. Spacey SD, Szczygielski BI, Young SP, et al. Malaysian siblings with Friedreich ataxia and chorea: a novel deletion in the frataxin gene. Can J Neurol Sci 2004;31:383–6
10. Zhu D, Burke C, Leslie A, et al. Friedreich's ataxia with chorea and myoclonus caused by a compound heterozygosity for a novel deletion and the trinucleotide GAA expansion. Mov Disord 2002;17:585–9
11. Koeppen AH, Morral JA, Davis AN, et al. The dorsal root ganglion in Friedreich's ataxia. Acta Neuropathol 2009;118:763–76
12. Koeppen AH, Becker AB, Qian J, et al. Friedreich ataxia: hypoplasia of spinal cord and dorsal root ganglia. J Neuropathol Exp Neurol 2017; 76: 101–8
13. Morral JA, Davis AN, Qian J, et al. Pathology and pathogenesis of sensory neuropathy in Friedreich's ataxia. Acta Neuropathol 2010; 120: 97–108
14. Zühlke CH, Dalski A, Habeck M, et al. Extension of the mutation spectrum in Friedreich's ataxia: detection of an exon deletion and novel missense mutations. Eur J Hum Genet 2004; 12:979–82
15. Koeppen AH. Friedreich's ataxia: pathology, pathogenesis, and molecular genetics. J Neurol Sci 2011; 303:1–12